ELECTRONIC AND OPTICAL PROPERTIES OF THE SPINEL OXIDES $Mg_xZn_{1-x}Al_2O_4$ BY FIRST-PRINCIPLES CALCULATIONS

ELEKTRONSKE IN OPTIČNE LASTNOSTI SPINELNIH OKSIDOV $Mg_xZn_{1-x}Al_2O_4$, IZPELJANE IZ TEORETIČNIH OSNOV

Chao Xiang[1], Jianxiong Zhang[1], Yun Lu[2], Dong Tian[3], Cheng Peng[1]

[1]Yangtze Normai University, School of Mechanical and Engineering, Fuling 408000, China
[2]Chiba University, Institute of Material Science and Engineering, Chiba 2790000, Japan
[3]Kunming University of Science and Technology, Faculty of Science, Kunming 650093, China
1254618608@qq.com

The structural, electronic and optical properties of perfect $Mg_xZn_{1-x}Al_2O_4$ oxides have been studied by first-principles calculations within the generalized gradient approximation of the density functional theory. It is interesting to note that a linear increase of cell volume (V) with increasing doping amount (x) occurs. The band gap increases in the series from 3.851 eV to 5.079 eV, which is in agreement with theoretical and experimental values. In addition, a blue shift of the absorption shoulder is observed in the UV region with the increase of x, as predicted by the imaginary part $\varepsilon_2(\omega)$ of the dielectric function at zero frequency as well as bandgap. This can be explained by the threshold of the electronic transition from O-2p to the empty Mg-3p electron states due to the substitution of Zn with Mg. The real part $\varepsilon_1(\omega)$ of the dielectric function located at zero frequency has a square fit relationship with refractive index n(0), which is 1.71–1.77 from x=0 to x=1. The energy-loss function shows that the replacement of Zn by Mg is responsible for a decrease in the intensity of the sharp peaks. The reflectivity shows that a higher coefficient of reflectivity (R(0)) at zero frequency corresponds to a smaller bandgap.

Keywords: electronic transitions, dielectric function, refractive index, adsorption shoulder

Preiskovali smo strukturne, elektronske in optične lastnosti idealnih $Mg_xZn_{1-x}Al_2O_4$ oksidov, izpeljane iz teoretičnih osnov znotraj posplošene gradientne aproksimacije funkcionalne teorije gostote. Opazili smo linearno povečanje celičnega volumna (V) z naraščajočo koncentracijo Mg (x). Širina prepovedanega pasu narašča od 3.851 eV to 5.079 eV v skladu s teoretičnimi in eksperimentalnimi vrednostmi. Poleg tega ob naraščanju deleža Mg opazimo modri premik dodatnega absorpcijskega vrha v UV območju, kakor napovedujeta vrednosti imaginarnega dela $\varepsilon_2(\omega)$ dielektrične funkcije pri frekvenci 0 in prepovedanega pasu. To je mogoče pojasniti s pragom elektronskega prehoda elektronov iz O-2p v prazen Mg-3p zaradi nadomestitve Zn z Mg. Kvadrat realnega dela $\varepsilon_1(\omega)$ dielektrične funkcije pri frekvenci 0 se ujema z lomnim količnikom n(0), ki je 1.71–1.77 za x=0 do x=1. Funkcija izgube energije, kaže, da zamenjava Zn z Mg povzroča zmanjšanje intenzitete ostrih vrhov. Reflektivnost kaže, da višji koeficient refleksije (R(0)) pri frekvenci 0 odgovarja manjši širini prepovedanega pasu.

Ključne besede: prehodi elektronov, dielektrična funkcija, lomni količnik, dodatni absorpcijski vrh

1 INTRODUCTION

Spinal oxides with the general chemical formula AB_2O_4 have a close-packed, face-centered-cubic structure (space group $Fd\bar{3}m$) characterized by two symmetrically distinct polyhedra: a tetrahedron and an octahedron. They are widely used in various fields such as catalysis, gas sensor, semiconductor, biomedical, catalyst carrier, as well as electroluminescent displays owing to their catalytic, physical, structural, electronic and optical properties.[1,2] Among them, $MgAl_2O_4$ and $ZnAl_2O_4$ have high-temperature resistance,[3,4] and they are highly reflective for wavelengths in the ultraviolet (UV) region, which make them candidate materials for reflective optical coating in aerospace applications.[5] In particular, $MgAl_2O_4$ is one of the potential candidates for the full wave band transparent window materials with high transmittance in IR- and visible-wavelength even extending to microwave ranges,[6,7] and it also can be used as lamps and lasers,[8] transparent ceramic material for high-temperature,[9] transparent armor and glass.[10]

Similarly, $ZnAl_2O_4$ can be used as a ceramic material similar to $MgAl_2O_4$. It can be used as a transparent conductor, optical material and dielectric material,[11,12] and it is suitable for UV photoelectronic applications.[13] Simultaneously, much work has been done on the structural, electronic and optical properties of $MgAl_2O_4$ and $ZnAl_2O_4$ over the past few years.[14–27] The effect of point vacancies on the spectral properties of $MgAl_2O_4$ has been studied by S. L. Jiang et al.[14] They revealed that the absorption peak at 5.3 eV is attributed to the neutral oxygen vacancy V_o^0, while two peaks at 3.2 eV and 4.75 eV are attributed to the 1+ charged oxygen vacancy V_o^{1+}. A related mechanism of transparency in $MgAl_2O_4$ nanoceramics prepared by sintering under high pressure and low temperature has been studied by J. Zhang et al.[15], who suggested that the decrease in the transparency with increasing temperature (>700 °C) is therefore a result of the light scattering at large pores. The low-temperature, high-pressure preparation of transparent nanocrystalline $MgAl_2O_4$ ceramics has been investigated by T. C. Lu et

MATERIALI IN TEHNOLOGIJE/MATERIALS AND TECHNOLOGY (1967–2017) – 50 LET/50 YEARS

C. XIANG et al.: ELECTRONIC AND OPTICAL PROPERTIES OF THE SPINEL OXIDES ...

al.,[16] indicating that the nanoceramics are highly transparent even though their relative densities are all less than 99 %, owing to the low or negligible light scattering from the nanosized grains and pores. The optical properties of $ZnAl_2O_4$ nanomaterials obtained by the hydrothermal method have been investigated by Miron and co-workers,[17] demonstrating that the band gap is determined from the absorbance spectra, and it depends strongly on the temperature used for further heating the samples. A first-principles study on structural, electronic and optical properties of spinel oxides $ZnAl_2O_4$, $ZnGa_2O_4$ and $ZnIn_2O_4$ has been carried out by F. Zerarga and co-workers,[18] implying that the peaks and structures in the optical spectra are assigned to interband transitions. The fabrication of transparent polycrystalline $ZnAl_2O_4$ – a new optical bulk ceramic – has been investigated by Goldstein and co-workers[19], who suggested that specimens have a high transparency (ILT≈78\%; λ = 800 nm; t = 2 mm). Plus, the differences in structural, electronic and optical performance between aluminum spinel $MgAl_2O_4$ and $ZnAl_2O_4$ have been presented.[28–30] To the best of our knowledge, the structure, electronic and optical properties of $Mg_xZn_{1-x}Al_2O_4$ (0<x<1), expressed quantitatively, which is that Zn^{2+} of $ZnAl_2O_4$ is replaced by Mg^{2+}, has not been investigated. The main aim of this investigation is to study the effect of the replacement of Zn by Mg on the structural, electronic and optical properties of $ZnAl_2O_4$.

2 MODEL AND COMPUTATIONAL DETAILS

In our calculations a 56-atom unit cell was modeled for the investigation of spinel $Mg_xZn_{1-x}Al_2O_4$ in **Figure 1**. All the calculations were performed using the Cambridge Serial Total Energy Package (CASTEP) program,[31] based on density functional theory (DFT).
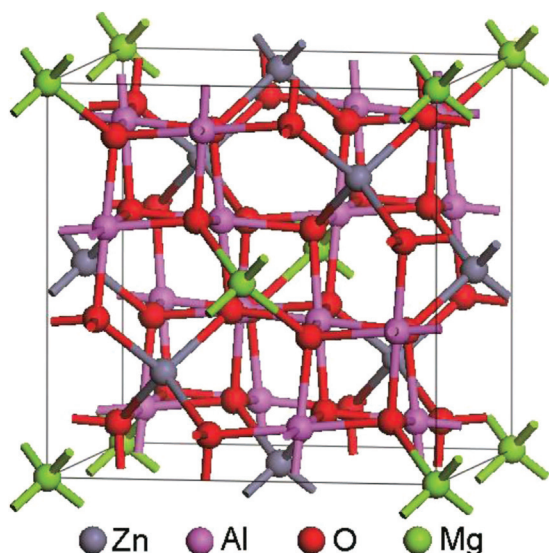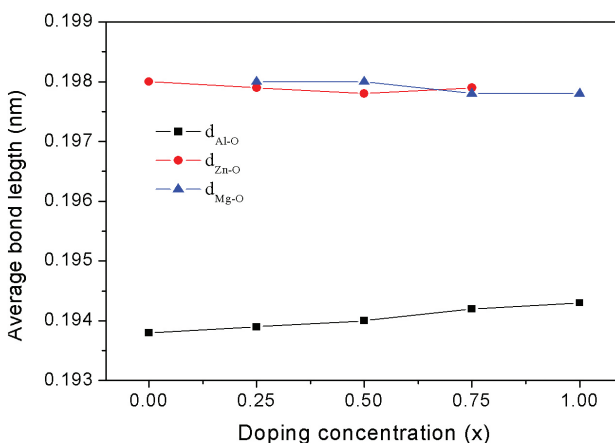
Electron-ion interaction for cations and anions was described by the ultra-soft pseudo-potential. The Mg-3s and -3p, Zn-3d and -4s, Al-3s and -3p, as well as O-2s and -2p states were treated as valence electrons. The exchange-correlation potential was calculated by the generalized gradient approximation (GGA) developed by the Perdew, Burke, and Ernzerhof functional (PBE).[32] The Engel-Vosko scheme (GGA+U) was applied to electronic properties calculations.[33] The on-site Coulomb Hubbard interaction U = 1 eV is used to treat correctly the localized 3d electrons in the $Mg_xZn_{1-x}Al_2O_4$. The unit cell was optimized using the Broyden, Fletcher, Goldfarb, Shanno (BFGS) method,[34] and convergence tolerance of energy charge, maximum force and stress were 1×10^{-5} eV, 0.03 eV/nm, and 0.05 GPa, respectively.[18,35] The plane-wave basis set cutoff energy was set to 340 eV.[18,35,36] The Brillouin-zone integration was implemented within Monkhorst-Pack scheme using a 4×4×4 mesh to optimize structures and calculate the electronic and optical properties.

3 RESULTS AND DISCUSSION

3.1 Structure and electronic properties

To obtain the stable structure of $Mg_xZn_{1-x}Al_2O_4$ spinel, the internal coordinates and lattice parameters of crystals were relaxed during geometry optimization. Structure parameters such as average bond lengths, cell volumes and lattice constants are presented, in comparison with the experimental data and values available from other calculations. As can be seen from **Tables 1** and **2**, the calculated equilibrium lattice constants a_0 of both $ZnAl_2O_4$ and $MgAl_2O_4$ are larger than the experimental values with less than 2 % deviation. Plus, substitution of Zn with Mg causes a slight increase in the lattice constant of $ZnAl_2O_4$. This is in agreement with the previous report.[28] In addition, one can see that the substitution of Zn with Mg is responsible for the formation of the pseudo-cubic, spinel-type structure. The average bond lengths of d_{Al-O} increases with increasing doping con-

Figure 1: $Mg_xZn_{1-x}Al_2O_4$ crystal structure. The gray, pink, green and red represent Zn, Al, Mg and O atoms, respectively.

Figure 2: Calculated average bond length (nm) of $Mg_xZn_{1-x}Al_2O_4$

MATERIALI IN TEHNOLOGIJE/MATERIALS AND TECHNOLOGY (1967–2017) – 50 LET/50 YEARS

C. XIANG et al.: ELECTRONIC AND OPTICAL PROPERTIES OF THE SPINEL OXIDES ...

centration (from $x=0$ to $x=1$) in **Figure 2**. In contrast, both d_{Zn-O} and d_{Mg-O} are nearly unchanged. This suggests that the increase of lattice constants is mostly due to an increase of d_{Al-O}. The minimum d_{Al-O} in $MgAl_2O_4$ is 0.1938 nm, which indicates that the strength of the chemical bond (Al-O) of $MgAl_2O_4$ is stronger than that of $Mg_xZn_{1-x}Al_2O_4$. The cell volume (V) is listed in **Table 2**. The volume-x curve is plotted, where x is the concentration of Mg. It is interesting to note that the unit-cell volume (V) changes linearly with the doping amount x (**Figure 3**).

Table 1: Calculated structure parameters for $Mg_xZn_{1-x}Al_2O_4$ ($x=0$, $x=1$), experimental measurement and other available theoretical values
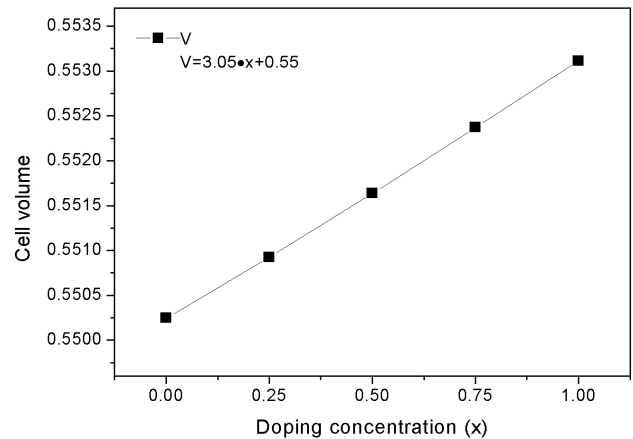
	$ZnAl_2O_4$			$MgAl_2O_4$		
	Present	Expt.	Calc.	Present	Expt.	Calc.
a_0 (nm)	0.8194	0.80911[37]	0.8032[18]	0.8208	0.80836[43]	0.8027[28]
			0.7995[28]		0.80844[44]	0.81074[25]
		0.8086[38]	0.8193[39]			0.814627m
			0.80215[40]		0.806[45]	0.80934[14]
			0.8018[41]			0.82[46]
			0.802[42]			

The calculated band gaps are presented in **Figure 4**. From the figure it is easy to see that the bottom of the conduction band and the top of the valence band for $Mg_xZn_{1-x}Al_2O_4$ occurs at Γ point with a direct band gap. Among them, $ZnAl_2O_4$ ($x=0$) has a band gap value of 3.851 eV, which is very close to the experimental value.[48] The $MgAl_2O_4$ ($x=1$) has a band gap value of 5.079 eV, which is underestimated with respect to the experimental value of 7.8 eV.[49] A similar issue has been addressed in previous theoretical calculations for $MgAl_2O_4$ such as 5.30 eV[14], 5.1 eV[27] and 5.36 eV.[28] This is mostly due to the fact that the calculated band gaps are related to DFT limitations, not considering the discontinuity in the exchange-correlation potential,[50] as mentioned in [35]. The calculations also show that the band-gap value increases due to changing the cation Zn with Mg. The band gap is 4.078 for $x=0.25$, 4.349 for $x=0.50$ and 4.638 eV for $x=0.75$.
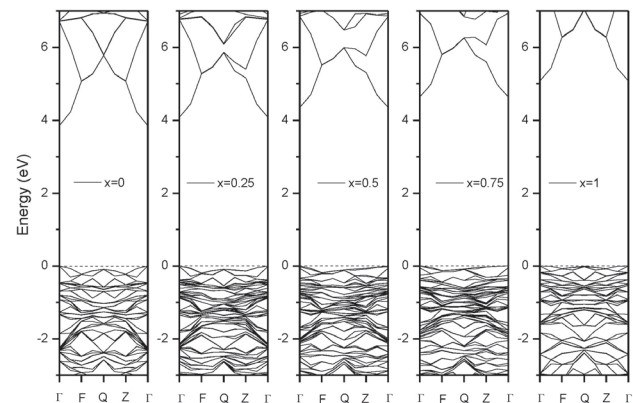
As discussed above, the band gap of optimized $Mg_xZn_{1-x}Al_2O_4$ is different (from $x=0$ to $x=1$). This is attributed to the difference in the density of states (DOS). To further elucidate the nature of the electronic band structure, we calculated the total density of states
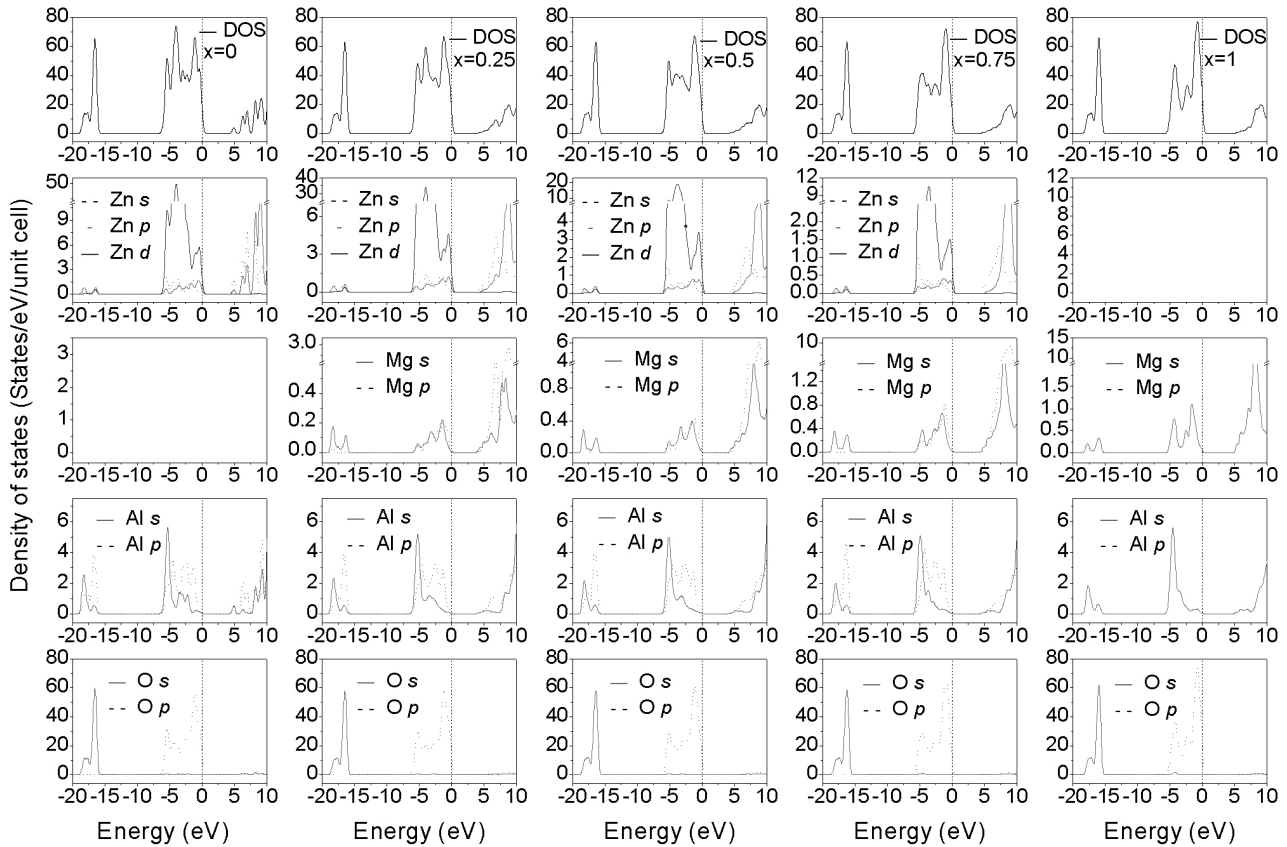

Figure 3: Calculated the unit cell volume V (nm^3) as a function of composition x

Figure 4: Calculated electronic band structure of $Mg_xZn_{1-x}Al_2O_4$ ($x=0$, $x=0.25$, $x=0.5$, $x=0.75$, $x=1$)

(DOS) and partial density of states (PDOS) of O, Zn, Mg and Al for the spinel oxides. As can be seen from **Figure 5**, the Fermi level is set to zero. It is mostly created by Zn-3d and O-2p states for $x=0$, with small contributions coming from Al-3p, and it is mostly created by Mg-3p and O-2p states for $x=1$, with small contributions of Al-3p. The character of the upper valence band is localized between -6.2 eV and 0 eV, which is mainly due to hybridization between the Zn-3d and O-2p states and due less to hybridization of O-2p with Zn-3p, Zn-4s, Mg-3s, Mg-3p, Al-3s and Al-3p as well. The lower valence band in the energy range -18.8 eV to -16.3 eV is

Table 2: Calculated structure parameters for $Mg_xZn_{1-x}Al_2O_4$

	0.000			0.250	0.500	0.750	1000		Al_2O_3
a(nm)	0.8194			0.8198	0.8202	0.8205	0.8208		
b(nm)	0.8194			0.8197	0.8202	0.8205	0.8208		
c(nm)	0.8194			0.8197	0.8199	0.8203	0.8208		
d_{Zn-O}(nm)	0.1980	0.2019[18]		0.1979	0.1978	0.1979		0.2032[18]	
d_{Al-O}(nm)	0.1938	0.1963[18]	0.188[b]	0.1939	0.1940	0.1942	0.1943	0.19419[25]	0.192[47]
d_{Mg-O}(nm)				0.1980	0.1980	0.1978	0.1978	0.19569[25]	
Volume (nm^3)	550.25			0.55092	0.55164	0.55237	0.55312		

MATERIALI IN TEHNOLOGIJE/MATERIALS AND TECHNOLOGY (1967–2017) – 50 LET/50 YEARS

C. XIANG et al.: ELECTRONIC AND OPTICAL PROPERTIES OF THE SPINEL OXIDES ...

Figure 5: Calculated total (DOS) and partial densities (PDOS) of states for $Mg_xZn_{1-x}Al_2O_4$ (x=0, x=0.25, x=0.5, x=0.75, x=1)

mostly attributed to the O 2s states which split into two: a sharp peak at -17.8 eV and a lower part 2.3 eV wide with double peaks for x=0. A similar issue appears for x=1, from which we can see that the lower valence band located at approximately -15.4 eV – -18.1 eV is mostly due to the O 2s states, which split into two: a sharp peak at -16.1 eV and a lower double peak with a width of 2.1 eV. This is in agreement with other theoretical calculations.[14,25] Moreover, we note that Zn-4s and Al-3p states play the main role in the conduction band above the Fermi level (between 3.8 eV and 8.2 eV) for x=0, while conduction band is mainly created by Mg-3p states for x=1.

3.2 Optical properties

The common response from both electronic and ionic polarization are taken into account in the condition of a low-frequency electric field, although only electronic polarization is considered as the dielectric function, and phonon contributions to the optical is not taken into account, when calculating optical properties in CASTEP package. It is well known that the optical properties are determined considering only direct interband transitions. One of the main optical characteristics of a solid is its dielectric function, which can express other optical properties and describe the optical response of the medium. The dielectric function, $\varepsilon(\omega)$, is given in Equation (1):

$$\varepsilon(\omega) = \varepsilon_1(\omega) + \varepsilon_2(\omega) \qquad (1)$$

Here $\varepsilon_1(\omega)$ and $\varepsilon_2(\omega)$ are the real and imaginary parts of the dielectric function, respectively. The complex $\varepsilon_2(\omega)$ is defined as Equation (2):[39]

$$\varepsilon_2(\omega) = \frac{2e^2\pi}{V\varepsilon_0} \sum_{k,v,c} \left| \left\langle \varphi_k^c | u \cdot r | \varphi_k^v \right\rangle \right|^2 \delta(E_k^c - E_k^v - \hbar\psi) \quad (2)$$

where V is the unit cell volume, u is the vector defining the polarization of the incident electric field, c and v are the valence band and conduction band, respectively, r is the momentum operator, and both E_k^c and E_k^v are eigenstates. This expression is similar to Fermi's golden rule for time-dependent perturbations. The $\varepsilon_2(\omega)$ can be thought of as detailing the real transitions between the unoccupied and occupied electronic states. The imaginary and real parts of the dielectric function are linked by a Kramers-Kronig transform because the dielectric function describes a causal response. Furthermore, the Kramers-Kronig transform is also used to obtain the $\varepsilon_1(\omega)$, which is:[18]

$$\varepsilon_1(\omega) = 1 + \frac{2}{\pi} P \int_0^\infty \frac{\omega' \varepsilon_2(\omega')}{(\omega')^2 - (\omega)^2} d\omega' \qquad (3)$$

Both imaginary parts and the real of the dielectric function can also be used to calculate important optical

MATERIALI IN TEHNOLOGIJE/MATERIALS AND TECHNOLOGY (1967–2017) – 50 LET/50 YEARS

C. XIANG et al.: ELECTRONIC AND OPTICAL PROPERTIES OF THE SPINEL OXIDES ...

functions, such as the refractive index $n(\omega)$ and the reflectivity $R(\omega)$:[18]

$$n(\omega) = \left[\frac{\varepsilon(\omega)}{2} + \frac{\sqrt{\varepsilon_1^2(\omega) + \varepsilon_2^2(\omega)}}{2} \right]^2 \qquad (4)$$

$$R(\omega) = \left[\frac{\varepsilon(\omega)^{0.5} - 1}{\varepsilon(\omega)^{0.5} + 1} \right]^2 \qquad (5)$$

The peak of the imaginary part of the dielectric function corresponds to electronic transitions from the valence to conduction bands, depending on the electronic transition energy of the conduction and valence band, i.e., the band-gap energies. The instrumental smearing of 0.3 eV is used to simulate the broadening effects. The dielectric functions for various x are displayed in **Figure 6**. It can be seen that the first critical point starts at (3.49, 3.61, 3.90, 4.22 and 4.63) eV from $x=0$ to $x=1$. These are known as the edge of the optical absorption. Furthermore, the different widths of the non-zero part of $\varepsilon_2(\omega)$ are related with different widths of the adsorption spectra, as shown in **Figure 6**, suggesting that absorption region for $Mg_xZn_{1-x}Al_2O_4(x=0)$ is wider than that of $Mg_xZn_{1-x}Al_2O_4\}(x=1)$. Other peak locates at (7.38, 10.87, 14.63 and 15.54) eV for $x=0$, (7.49, 7.37, 11.65, 12.83 and 14.22) eV for $x=0.25$, (6.83, 7.84, 10.31, 12.81 and 15.36) eV for $x=0.5$, (5.81, 10.16, 12.85 and 15.85) eV for $x=0.75$ and (6.25, 7.69, 10.01, 12.91 and 16.16) eV for $x=1$, in comparison with other theoretical values listed in **Table 3**. These peaks of origins and features on

the basis of decomposing each spectrum to its individual pair contribution from each pair of valence and conduction bands are obtained by the analysis of $\varepsilon_2(\omega)$.[18] The calculated real part of $\varepsilon_1(\omega)$ in infinite wavelength (i.e., the limit of zero energy) for $x=0$ is 3.15 and for $x=1$ is 2.93, which are in agreement with previous theoretical values such as 2.6691 for $ZnAl_2O_4$[18] and 3.112 for $MgAl_2O_4$.[25] In addition, the $\varepsilon_1(\omega)$ in infinite wavelength is 3.09 for $x=0.25$, 3.03 for $x=0.5$, and 2.98 for $x=0.75$, signaling a negative trend with the increase of the doping amount x. These can also indicate that the real part $\varepsilon_1(\omega)$ of the limit of zero energy has a square fit relationship with the refractive index n localized zero energy. The $\varepsilon_1(\omega)$ reaches a maximum value of 4.22 at about 6.15 eV for $x=0$, 4.28 at 8.88 eV for $x=0.25$, 4.30 at 8.82 eV for $x=0.5$, 4.29 at 8.84 eV for $x=0.75$ and 4.39 at 8.73 for $x=1$.

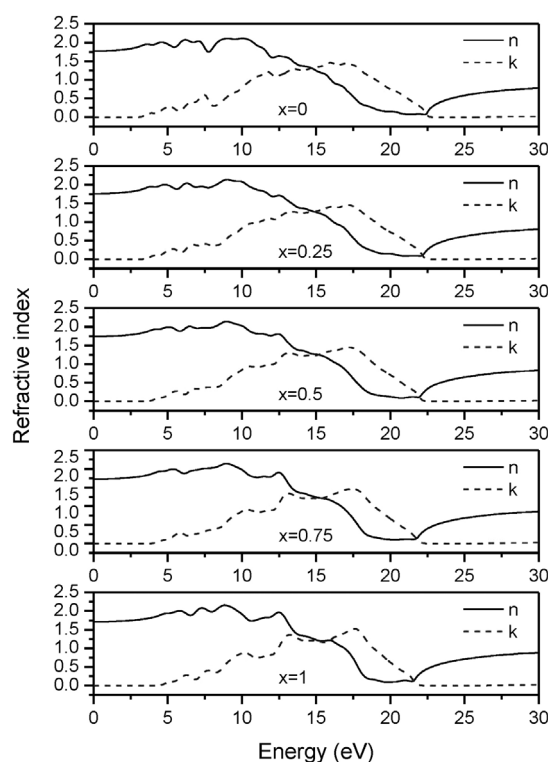**Table 3:** The imaginary part ($\varepsilon_2(\omega)$) of dielectric function for $Mg_xZn_{1-x}Al_2O_4$ ($x=0$, $x=1$).

	ZnAl$_2$O$_4$			MgAl$_2$O$_4$		
	Present	Calc.[18]	Calc.[40]	Present	Calc.[23]	Calc.[25]
Threshold Peak position	3.49	4.31	~4.25	4.63	7.4	
	7.38	7.82	~8.01	6.25		6.27
	10.87	10.98		7.69		7.44
	14.63	14.08		10.01		9.42
	15.54			12.91		10.19

The refractive index and the extinction coefficient are shown in **Figure 7**. One can see that the static refractive
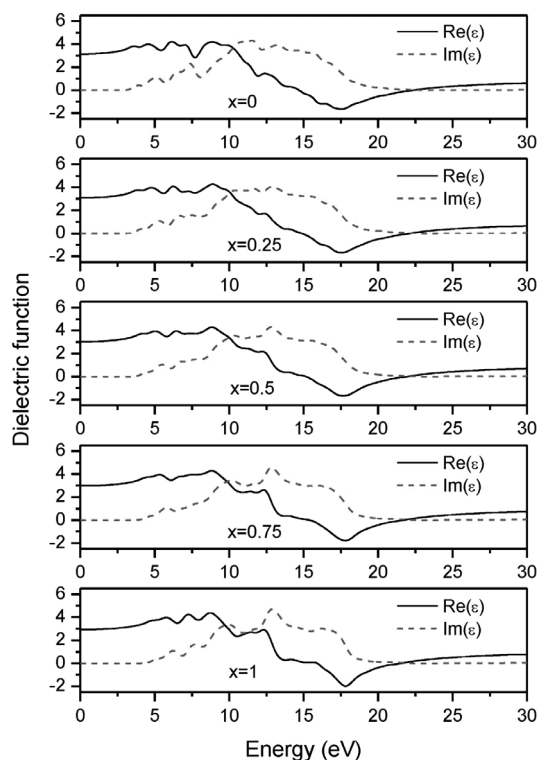
Figure 6: Dielectric function of Mg doped ions at different doping concentration

Figure 7: Refractive index of Mg doped ions at various doping concentration

MATERIALI IN TEHNOLOGIJE/MATERIALS AND TECHNOLOGY (1967–2017) – 50 LET/50 YEARS

C. XIANG et al.: ELECTRONIC AND OPTICAL PROPERTIES OF THE SPINEL OXIDES ...

index $n(0)$ at the zero frequency limits is 1.77, 1.76, 1.73, 1.72 and 1.71 from $x=0$ to $x=1$, which are consistent with values derived from the real part $\varepsilon_1(\omega)$ of the dielectric function mentioned above. They reach a maximum value of 2.12 at 10.05 eV for $x=0$, 2.14 at 9.01 eV for $x=0.25$, 2.13 at 8.97 eV for $x=0.5$, 2.14 at 8.95 ev for $x=0.75$ and 2.16 at 8.84 eV for $x=1$, compared to other theoretical values listed in **Table 4**. We note that the refractive index $n(0)$ decreases with an increase of x. It indicates that the $n(0)$ likely is decided by the bond length of Zn-O, Al-O, Mg-O and the volume of $Mg_xZn_{1-x}Al_2O_4$.

Table 4: Calculated refractive index for $Mg_xZn_{1-x}Al_2O_4$ ($x=0$, $x=1$)

| | $n(0)$ | n | |
		Maximum	Energy(eV)
$ZnAl_2O_4$			
Present	1.77	2.13	10.15
Calc.	1.63	2.16	10.71
Calc.	1.74		
$MgAl_2O_4$			
Present	1.71	2.16	8.84
Calc.[53]	1.61	2.40	11.35
Calc.[25]	1.763		
Expt.[54]	1.71		

The different band structure is responsible for different structure in the optical spectra because the optical spectra originates from the transitions from the top valence band to the bottom conduction band. For instance, a different band gap corresponds to different absorption edge. The relationship between the absorption edge and the band gap is described by Equation (6):

$$\left(\frac{hc}{\lambda}\right)^2 \left(\frac{1}{d}\right)^2 \ln^2\left(\frac{1}{T}\right) = A\left(\frac{hc}{\lambda} - E_g\right) \tag{6}$$
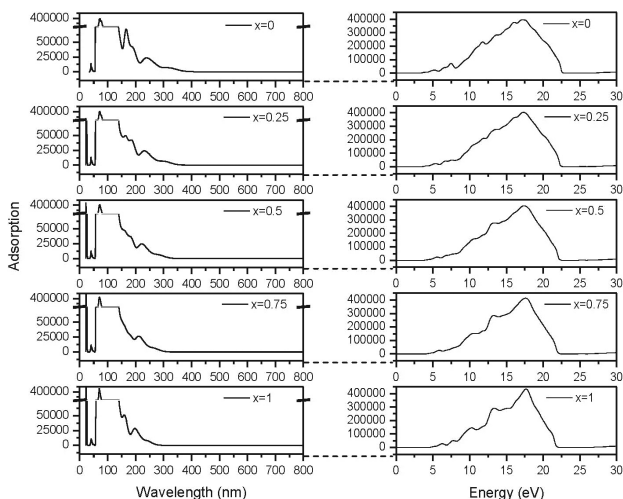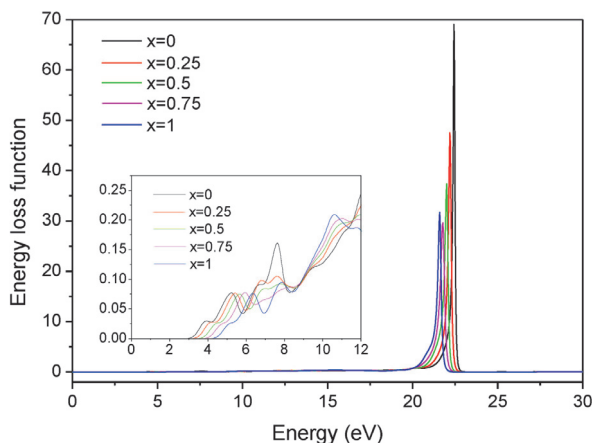

Figure 8: Absorption spectra of Mg doped ions at various doping concentration: a) the unit of the vertical axis for absorption spectra is wavelength (nm), b) the unit of abscissa is energy (eV)

where λ is the wavelength, T is the transmissivity, A is the transition coefficients of the direct band gap, d is the thickness and E_g is the value of the band gap. As shown in **Figure 8a**, it is found that $Mg_xZn_{1-x}Al_2O_4(x=0)$ shows an absorption shoulder around 360 nm, which is in agreement with the experimental value. For instance, the optical absorbance spectrum of $ZnAl_2O_4$ was detected in the 250–400 nm region at room temperature,[17] and its adsorption shoulder was also observed in the 290–375 nm wavelength region for the sample calcined at 700 °C.[52] $Mg_xZn_{1-x}Al_2O_4(x=1)$ shows an absorption shoulder around 270 nm, meaning that the absorption shoulder undergoes a small blue shift. This is in agreement with the imaginary part $\varepsilon_2(\omega)$ of the dielectric function, and also suggests that perfect $MgAl_2O_4$ spinel is a transparent crystal, and its transparency is higher than that of $ZnAl_2O_4$ in the visible region. Meanwhile, the absorption shoulder is 340 nm for $x=0.25$, 310 nm for $x=0.50$, 290 nm for $x=0.75$ and 270 nm for $x=1$. Moreover, as shown in **Figure 8b**, where it seems that the absorption region shifts towards lower energy for $ZnAl_2O_4$ than $MgAl_2O_4$ due to the smaller band gap of the former than the latter, as predicted by the imaginary part of the dielectric function as well as the data derived from Equation (6). The absorption edge starts from about (3.66, 3.95, 4.18, 4.50 and 4.86) eV from $x=0$ to $x=1$. This is mainly attributed to electronic transitions from the O-2p located at the top of the valence band to the empty Zn-4s electron states dominating the bottom of the conduction band for $x=0$. Since Zn is replaced by Mg, electronic transitions from O-2p to the empty Mg-3p electron states, yielding an increase in band gap, so that absorption edge starts at higher energy (4.86 eV), due to Mg-3p electron states dominating the bottom of the conduction band for $x=1$. Other peaks locates at (7.46, 11.77, 13.80, 16.05 and 17.15) eV for $x=0$, (6.75, 7.57, 11.91, 13.63 and 17.30) eV for $x=0.25$, (5.61, 13.41 and 17.35) for $x=0.5$, (5.85, 10.49, 13.21 and 17.58) eV for $x=0.75$ and (6.28, 7.76, 10.21, 13.33, 15.11 and 17.66) eV for $x=1$, in comparison with other theoretical values listed in **Table 5**.

Table 5: The adsorption spectra of perfect $Mg_xZn_{1-x}Al_2O_4$ ($x=0$, $x=1$).

| | $ZnAl_2O_4$ | | | $MgAl_2O_4$ | |
	Present	Calc.[18]	Calc.[40]	Present	Calc.[14]
Threshold Peak position	3.66	4.20	~4.31	4.86	~5.05
	7.46	7.83	~8.03	6.28	~6.14
	13.80	14.17		7.76	~7.03
	16.05	16.41		10.21	~10.15
	17.15	17.35		13.33	13.75

The energy-loss function has a large effect on usage of material. For example, the sharper peak of energy loss, explained narrower scope, the better the optical storage efficiency. Besides, energy loss function is an important factor for describing the energy loss of a fast electron traversing in a material, and the prominent

MATERIALI IN TEHNOLOGIJE/MATERIALS AND TECHNOLOGY (1967–2017) – 50 LET/50 YEARS

C. XIANG et al.: ELECTRONIC AND OPTICAL PROPERTIES OF THE SPINEL OXIDES ...

Figure 9: Calculated energy loss function of $Mg_xZn_{1-x}Al_2O_4$ obtained from the CASTEP calculations
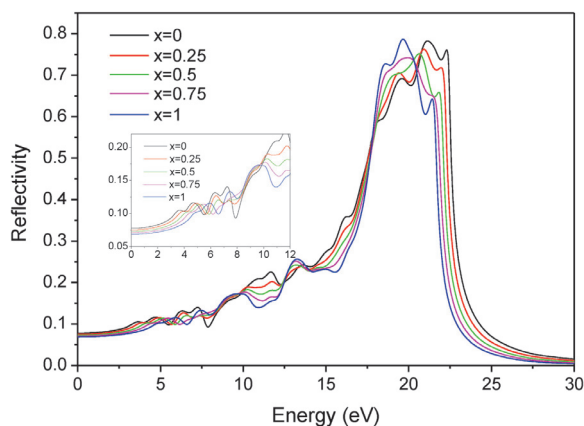
Figure 10: Calculated reflection of $Mg_xZn_{1-x}Al_2O_4$ obtained from the CASTEP calculation

peaks in the energy-loss function representing a characteristic associated with the plasma resonance (a collective oscillation of the valence electrons).[51] The energy-loss function is displayed in **Figure 9**. It can be seen that the primary peak emerges at 22.43 eV for x=0 ($ZnAl_2O_4$), which is consistent with the theoretical value of 20.99 eV.[18] Additionally, the energy-loss function for $ZnAl_2O_4$ between 0 eV and 12 eV is in agreement with a previous report.[40] Other peaks are located at 22.19 eV for x=0.25, 22.00 eV for x=0.5, 21.78 eV for x=0.75 and 21.60 eV for x=1.

There is close relationship between reflectivity and band gap, i.e., the higher coefficient of reflectivity ($R(0)$) at zero frequency corresponds to a smaller band gap. Additionally, the reflection takes an important role in optical losses. As can be seen from **Figure 10** the high reflectivity localizes between 18.61 eV and 22.32 eV, which is consistent with the energy-loss function mentioned above.

4 CONCLUSIONS

The effect of Mg^{+2} versus Zn^{+2} by comparing the structural, electronic and optical properties of $Mg_xZn_{1-x}Al_2O_4$ (from x=0 to x=1) has been implemented using the DFT+U method. The calculations show that the volume of the unit cell changes linearly with increasing Mg-doping amount (x). The Al-O bond length of $Mg_xZn_{1-x}Al_2O_4$ increases with x, suggesting it has a weaker bond stiffness. On the basis of the imaginary parts of the dielectric function, it is found that critical points occur at about 3.49 eV for $ZnAl_2O_4$, which is lower than that for Mg-doped $ZnAl_2O_4$, indicating that absorption shoulder undergoes a blue shift in the UV region as evidenced by the absorption spectra. The blue shift is probably due to the electronic transition from O-2p to the empty Mg-3p electron states. For real parts of dielectric function, the limit of zero energy has a square fit relationship with the refractive index ($n(0)$) localized zero energy, which is verified by the reflectivity spectra. Furthermore, the absorbance spectra, reflectivity spectra and the refractive index show that these compounds are suitable for UV reflective coatings. The peak of the energy-loss function shows that $Mg_xZn_{1-x}Al_2O_4$ can be a candidate for optical storage materials.

Acknowledgment

6 REFERENCES

[1] N. Bouropoulos, I. Tsiaoussis, P. Poulopoulos, P. Roditis, S. Baskoutas, ZnO controllable sized quantum dots produced by polyol method: an experimental and theoretical study, Mater. Lett., 62 (**2008**), 3533–3535, doi:10.1016/j.matlet.2008.03.044

[2] W. S. Tzing, W. H. Tuan, The strength of duplex Al_2O_3-$ZnAl_2O_4$ composite, J. Mater. Sci. Lett., 15.16 (**1996**), 1395–1396, doi:10.1007/BF00275286

[3] S. A.T. Redfen, R. J. Harrison, H. S. C. O'Neill, D. R. R. Wood, Thermodynamics and kinetics of cation ordering in $MgAl_2O_4$ spinel up to 1600 °C from in situ neutron diffraction, Amer. Mineral., 84.3 (**1999**), 299–310, doi:10.2138/am-1999-0313

[4] H. Cynn, S. K. Sharma, T. F. Cooney, M. Nicol, High-temperature Raman investigation of order-disorder behavior in the $MgAl_2O_4$ spinel, Phys. Rev. B, 45.1 (**1992**), 500–502, doi:10.1103/PhysRevB.45.500

[5] QivaStar. Inc, Ridgeerest. CA, and Hugest Space and Communication CO., El. Segundo, CA, U. S. Pat. N0. 5820669, 1998

[6] K. P. Surendran, P.V. Bijumon, P. Mohanan, M.T. Sebastian, (1-x)$MgAl_2O_4$-$_x$$TiO_2$ dielectrics for microwave and millimeter wave applications, Appl. Phys., A 81.4 (**2005**), 823–826, doi:10.1007/s00339-005-3282-5

[7] P. Fu, W. Z. Lu, W. Lei, Y. Xu, X. H. Wang, J. M. Wu, Transparent polycrystalline MgAl2O4 ceramic fabricated by spark plasma sintering: Microwave dielectric and optical properties, Ceram. Int., 39.3 (**2013**), 2481–2487, doi:10.1016/j.ceramint.2012.09.006

MATERIALI IN TEHNOLOGIJE/MATERIALS AND TECHNOLOGY (1967–2017) – 50 LET/50 YEARS

C. XIANG et al.: ELECTRONIC AND OPTICAL PROPERTIES OF THE SPINEL OXIDES ...

[8] G. Gilde, P. Patel, P. Patterson, D. Blodgett, D. Hahn, Evaluation of hot pressing and hot isostatic pressing parameters on the optical properties of spinel, J. Am. Ceram. Soc., 88.10 (2005), 2747–2751, doi: 10.1111/j.1551-2916.2005.00527.x

[9] J. G. Li, T. Ikegami, J. H. Lee, T. Mori, Fabrication of translucent magnesium aluminum spinel ceramics, J. Am. Ceram. Soc., 83.11 (2000), 2866–2868, doi:10.1111/j.1151-2916.2000.tb01648.x

[10] W. Miao, Y. Wu, H. Zhou, W. Han, F. Ru, Low-temperature sintering of A1N ceramics with shock wave treated powder, Mater. Lett., 30.5-6 (1997), 411–414, doi:10.1016/s0167-577x(96)00232-7

[11] N. J. Van der Laag, M. D. Snel, P. C. M. M. Magusin, G. de With, Structural, elastic, thermophysical and dielectric properties of zinc aluminate (ZnAl$_2$O$_4$), J. Eur. Ceram. Soc., 24.8 (2004), 2417–2424, doi:10.1016/j.jeurceramsoc.2003.06.001

[12] X. Y. Chen, C. Ma, Spherical porous ZnAl$_2$O$_4$: Eu^{3+} phosphors: PEG-assisted hydrothermal growth and photoluminescence, Opt. Mater., 32.3 (2010), 415–421, doi:10.1016/j.optmat.2009.10.001

[13] Y. Wang, Q. Liao, H. Lei, X. P. Zhang, X.C. Ai, J. P. Zhang, K. Wu, Interfacial reaction growth: morphology, composition, and structure controls in preparation of crystalline Zn$_x$Al$_y$O$_z$ nanonets, Adv. Mater., 18.7 (2006), 943–947, doi:10.1002/adma.200502154

[14] S. L. Jiang, T. C. Lu, J. Zhang, First-principles study on the effects of point vacancies on the spectral properties of MgAl$_2$O$_4$, J. Chen, Solid State Commun., 151 (2011), 29–32, doi:10.1016/j.ssc.2010.10.030

[15] J. Zhang, T. C. Lu, X. H. Chang, N. Wei, W. Xu, Related mechanism of transparency in MgAl$_2$O$_4$ nano-ceramics prepared by sintering under high pressure and low temperature, J. Phys. D: Appl. Phys., 42 (2009) 052002 (5pp), doi:10.1088/0022-3727/42/5/052002

[16] T. C. Lu, X. H. Chang, J. Q. Qi, X. J. Luo, Low-temperature high-pressure preparation of transparent nanocrystalline Mg Al$_2$O$_4$ ceramics, Appl. Phys. Lett., 88.21 (2006), 213120, doi:10.1063/1.2207571

[17] I. Miron, C. Enache, M. Vasile, I. Grozescu, Optical properties of ZnAl$_2$O$_4$ nanomaterials obtained by the hydrothermal method, Phys. Scr., T149 (2012) 014064 (3pp), doi:10.1088/0031-8949/2012/T149/014064

[18] F. Zerarga, A. Bouhemadou, R. Khenata, S. Bin-Omran,Structural, electronic and optical properties of spinel oxides ZnAl$_2$O$_4$, ZnGa$_2$O$_4$ and ZnIn$_2$O$_4$, Solid State Sci., 13.8 (2011), 1638–1648, doi:10.1016/j.solidstatesciences.2011.06.016

[19] A. Goldstein, Y. Yeshurun, M. Vulfson, H. Kravits, Fabrication of transparent polycrystalline ZnAl$_2$O$_4$–a new optical bulk ceramic, J. Ceram. Soc., 95(2012) 3, 879–882, doi:10.1111/j.1551-2916.2011.05063.x

[20] S. L. Jiang, T. C. Lu, Y. Long, J. Chen, Ab initio many-body study of the electronic and optical properties of MgAl$_2$O$_4$ spinel, J. Appl. Phys. 111.4 (2012), 043516, doi:10.1063/1.3686727

[21] L. Zhang, G. F. Ji, F. Zhao, Z. Z. Gong, First-principles study of the structural, mechanical and electronic properties of ZnX$_2$O$_4$ (X=Al, Cr and Ga), Chin. Phys. B., 20 (2011), 4, doi:10.1088/1674-1056/20/4/047102

[22] C. Ragupathi, J. J. Vijaya, A. Manikandan, L. J. Kennedy, Phyto-synthesis of nanoscale ZnAl$_2$O$_4$ by using sesamum (Sesamum indicum L.) optical and catalytic properties, J. Nanosci. Nanotechno., 13 (2013) 12, 8298–8306, doi:10.1166/jnn.2013.7922

[23] M. Arbi, N. Benramdane, Z. Kebbab, R. Miloua, F. Chiker, First principles calculations of structural, electronic and optical properties of zinc aluminum oxide, Mater. Sci. Semicond. Process., 15 (2012) 3, 301–307, doi:10.1016/j.mssp.2012.03.010

[24] H. Dixit, N. Tandon, S. Cottenier, R. Saniz, D. Lamoen, B. Partoens, V. V. Speybroeck, M. Waroquier, Electronic structure and band gap of zinc spinel oxides beyond LDA: ZnAl$_2$O$_4$, ZnGa$_2$O$_4$ and ZnIn$_2$O$_4$, New J. Phys., 13.6 (2011) 063002 (11pp), doi:10.1088/1367-2630/13/6/063002

[25] S. M. Hosseini, Structural, electronic and optical properties of spinel MgAl$_2$O$_4$ oxide, phys. Status Solidi B 245.12 (2008), 2800–2807, doi:10.1002/pssb.200844142

[26] A. Goldstein, Correlation between MgAl$_2$O$_4$-spinel structure, processing factors and functional properties of transparent parts (progress review), J. Eur. Ceram. Soc. 32.11 (2012), 2869–2886, doi:10.1016/j.jeurceramsoc.2012.02.051

[27] D. L. Zhang, X. G. Xu, W. Wang, X. Zhang, H. L. Yang, Y. Wu, C. Z. Ma, Y. Jiang, Electronic structures of new tunnel barrier spinel MgAl$_2$O$_4$ first-principles calculations, Rare Metals 31.2 (2012), 112–116, doi:10.1007/s12598-012-0473-z

[28] R. Khenata, M. Sahnoun, H. Baltache, M. Réshak, A. H. Reshak, Y. Al-Douri, B. Bouhafs, Full-potential calculations of structural, elastic and electronic properties of MgAl$_2$O$_4$ and ZnAl$_2$O$_4$ compounds, Phys. Lett. A 344.2 (2005), 271–279, doi:10.1016/j.physleta.2005.06.043

[29] Y. Y. Jiang, J. W. Zhang, Z. Q. Hu, J. X. Liu, Synthesis and Visible Light Photocatalytic Activity of Spinel MAl$_2$O$_4$ (M= Mg, Zn, Cu), Appl. Mech. Mater. 455 (2014), 99–105, doi:10.4028/www.scientific.net/AMM.455.99

[30] F. Y. Zhang, Z. Zeng, J. Q. You, The Electronic and Optical Properties of Al$_2$O$_3$, MO, and MAl$_2$O$_4$ (M= Zn, Mg), J. Nanosci. Nanotechno, doi: 10 (2010), 5475–5478

[31] M. D. Segall, P. J. D. Lindan, M. J. Probert, C. J. Pickard, P. J. Hasnip, S. J. Clark, M. C. Payne, First-principles simulation: ideas, illustrations and the CASTEP code, J. Phys-Condens. Mat., 14 (2002), 2717–2743, doi:10.1088/0953-8984/14/11/301

[32] J. P. Perdew, K. Burke, M. Ernzerhof, Generalized gradient approximation made simple, Phys. Rev. Lett., 77.18 (1996), 3865–3868, doi:10.1103/PhysRevLett.77.3865

[33] E. Engel, S. H. Vosko, Exact exchange-only potentials and the virial relation as microscopic criteria for generalized gradient approximations, Phys. Rev. B, 47.20 (1993), 13164, doi:10.1103/PhysRevB.47.13164

[34] B. G. Pfrommer, M. Côté, S. G. Louie, M. L. Cohen, Relaxation of crystals with the quasi-Newton method, J. Comput. Phys., 131.1 (1997), 233–240, doi:10.1006/jcph.1996.5612

[35] M. G. Brik, First-principles calculations of electronic, optical and elastic properties of ZnAl 2 S 4 and ZnGa$_2$O$_4$, J. Phys. Chem. Solids, 71.10 (2010), 1435–1442, doi:10.1016/j.jpcs.2010.07.007

[36] A. Bouhemadou, R. Khenata, Pseudo-potential calculations of structural and elastic properties of spinel oxides ZnX$_2$O$_4$ (X = Al, Ga, In) under pressure effect, Phys. Lett. A 360 (2006) 2, 339, A. doi:10.1016/j.physleta.2006.08.008

[37] D. Errandonea, R. S. Kumar, F. J. Manjón, V. V. Ursaki, E. V. Rusu, Post-spinel transformations and equation of state in ZnGa$_2$O$_4$: determination at high pressure by in situ x-ray diffraction, Phys. Rev. B, 79.2 (2009), doi:10.1103/PhysRevB.79.024103

[38] R. J. Hill, J. R. Graig, G. V. Gibbs, Systematics of the spinel structure type, Physics and chemistry of minerals, Phys. Chem. Miner., 4 (1979), 317–339, doi:10.1007/BF00307535

[39] C. Xiang, H. L. Tan, J. S. Lu, Y. X. Yang, C. L. Ni, First-principles calculations of structural, electronic and optical properties of ZnGa$_x$Al$_{2-x}$O$_4$ spinel-type oxides, J. Alloys Compd. 581 (2013), 139–145, doi:10.1016/j.jallcom.2013.05.040

[40] S. Z. Karazhanov, P. Ravindran. Ab initio study of double oxides ZnX$_2$O$_4$ (X=Al, Ga, In) having spinel structure, J. Am. Ceram. Soc. 93 (2010), 3335–3341, doi:10.1111/j.1551-2916.2010.03864.x

[41] A. Seko, K. Yuge, F. Oba, A. Kuwabara, I. Tanaka, Prediction of ground-state structures and order-disorder phase transitions in II-III spinel oxides: A combined cluster-expansion method and first-principles study, Phys. Rev. 73.18 (2006), 184117, doi:10.1103/PhysRevB.73.184117

[42] S. López, A. H. Romero, First-principles study of the high-pressure phase transition in ZnAl$_2$O$_4$ and ZnGa$_2$O$_4$: From cubic spinel to orthorhombic post-spinel structures, Phys. Rev. B, 79 (2009), 21, doi:10.1103/PhysRevB.79.214103

[43] N. Kashii, H. Maekawa, Y. Hinatsu, Dynamics of the cation mixing of MgAl$_2$O$_4$ and ZnAl$_2$O$_4$ spinel, J. Am. Ceram. Soc., 82 (1999) 7, 1844–1848, doi:10.1111/j.1151-2916.1999.tb02007.x

MATERIALI IN TEHNOLOGIJE/MATERIALS AND TECHNOLOGY (1967–2017) – 50 LET/50 YEARS

C. XIANG et al.: ELECTRONIC AND OPTICAL PROPERTIES OF THE SPINEL OXIDES ...

[44] A. Navrotsky, B. A. Wechsler, K. Geisinger, F. Seifert, Thermochemistry of MgAl2O4-Al8/3O4 Defect Spinels, J. Am. Ceram. Soc., 69 (**1986**) 5, 418–422, doi:10.1111/j.1151-2916.1986.tb04772.x

[45] P. Fischer, Neutronenbeugungsuntersuchung der Strukturen von MgAl$_2$O$_4$-und ZnAl$_2$O$_4$-Spinellen, in Abhängigkeit von der Vorgeschichte, Z. Krist-Cryst. Mater., 124 (**1967**) 1–6, 275–302, doi:10.1524/zkri.1967.124.4-5.275

[46] H. Sukegawa, H. X. Xiu, T. Ohkubo, T. Furubayashi, T. Niizeki, W. H. Wang, S. Kasai, S. Mitani, K. Inomata, K. Hono, Tunnel magnetoresistance with improved bias voltage dependence in lattice-matched Fe/spinel MgAl 2 O 4/Fe (001) junctions, Appl. Phys. Lett. 96 (**2010**) 21, 212–505, doi:10.1063/1.3441409

[47] R. E. Newnham, Y. M. de Haan, Z. Kristallogr, Refinement of the a Al$_2$O$_3$, Ti$_2$O$_3$, V$_2$O$_3$ and Cr$_2$O$_3$ structures, Z. Krist-Cryst. Mater., 117.1–6 (**1962**), 235–237, doi:10.1524/zkri.1962.117.2-3.235

[48] S. K. Sampath, J. F. Cordaro, Optical properties of zinc aluminate, zinc gallate, and zinc aluminogallate spinels, J. Am. Ceram. Soc., 81 (**1998**) 3, 649–654, doi:10.1111/j.1151-2916.1998.tb02385.x

[49] M. L. Bortz, R. H. French, D. J. Jones, R.V. Kasowski, F. S. Ohuchi, Temperature dependence of the electronic structure of oxides: MgO, MgAl$_2$O$_4$ and Al$_2$O$_3$, Phys. Scr. 41 (**1990**), 537–541, doi:10.1088/0031-8949/41/4/036

[50] J. P. Perdew, M. Levy, Physical content of the exact Kohn-Sham orbital energies: band gaps and derivative discontinuities, Phys. Rev. Lett. 51 (**1983**) 20, 1884, doi:10.1103/PhysRevLett.51.1884

[51] M. Fox, Optical Properties of Solids. Academic Press, New York, 1972

[52] S. Mathur, M. Veith, M. Haas, H. Shen, N. Lecerf, V. Huch, Single-Source Sol-Gel Synthesis of Nanocrystalline ZnAl$_2$O$_4$: Structural and Optical Properties, J. Am. Ceram. Soc. 84 (**2001**), 1921–1928, doi:10.1111/j.1151-2916.2001.tb00938.x

[53] B. Amin, R. Khenata, A. Bouhemadou, Iftikhar Ahmad, M. Maqbool, Opto-electronic response of spinels MgAl$_2$O$_4$ and MgGa$_2$O$_4$ through modified Becke-Johnson exchange potential, Phy. B 407 (**2012**), 2588–2592,doi: 10.1016/j.physb.2012.03.075

[54] GEMSELECT, http://www.gemselect.com/gem-info/spinel/spinel-info.php, 1.10.2016